JEAS

Journal of Engineering and Applied Sciences 10 (2014), 6-18

JOURNAL OF ENGINEERING AND APPLIED SCIENCES

Analysis of excited rod on the Laplace variable domain

Ozoegwu C. G., Omenyi S. N.

Department of Mechanical Engineering, Nnamdi Azikiwe University, Awka

chigbogug@yahoo.com

Abstract

This work analyzes the continuum vibration of a uniform slender bar on the Laplace variable domain and validates the arising time response with the well-known time-domain analysis called the method of separation of variable. A novel form of the method of separation of variable is used alongside the popular form that assumes that the steady state response of the rod is of same form as the excitation to arrive at identical results that validate the presented s-domain analysis. Even though analysis is presented generally, a numerical case study is simulated and discussed. Both vibratory responses of displacement and stress are discussed. Possible application of method of this work is suggested to include the case of blades attached to an unbalanced shaft.

Keywords: Laplace transform, s-domain, continuum vibration, surface plot

1. Introduction

The popular lumped parameter analysis of elastic systems is analytical simplification of mathematical involvement of treating the systems as continuum. Most real elastic systems are continuous thus are of distributed parameter configuration. Vibration analysis of distributed elastic systems is important in design and sensitivity analysis of structures. Two types of vibration analysis of distributed parameter elastic systems are available. The first is the time domain approach to which the popular method of separation of variable [1-7] belongs. The other is the integral transform approach in which analysis is carried out in the transformed domain to get the transformed response that is retransformed in the time domain to get the time response. The lumped single degree of freedom (SDOF) case given below is treated as illustration. The harmonically forced and damped lumped SDOF is governed by the equation

$$\ddot{z}(t) + 2\xi\omega_n\dot{z}(t) + \omega_n^2 z(t) = F_0 e^{i\omega t} \tag{1}$$

The time domain analysis of steady state response of the system is carried out by inserting a solution of form $z(t) = Xe^{i\omega t}$ in equation (1) and solving to give the response

$$z(t) = \frac{F_0/k}{(1-\omega^2/\omega_n^2)+i2\xi\omega/\omega_n}\, e^{i\omega t} \tag{2}$$

The Laplace domain analysis of equation (1) is simply carried out by taking Laplace transform ignoring the initial conditions and simplifying to give

$$Z(s) = \frac{F_0}{(ms^2+cs+k)(s-i\omega)} \tag{3}$$

This is retransformed to give same result as in equation (2).

2. Mathematical Analysis of a Continuum Rod on s-domain

The longitudinal motion of a uniform slender bar is governed by the partial differential equation

$$\frac{\partial^2 u}{\partial t^2} = c^2 \frac{\partial^2 u}{\partial x^2} \tag{4}$$

Taking the Laplace transform of (4) with respect to t gives

$$\int_0^\infty c^2 \frac{\partial^2 u}{\partial x^2} e^{-st} dt = \int_0^\infty \frac{\partial^2 u}{\partial t^2} e^{-st} dt \tag{5}$$

Since differentiation in the left-hand-side (LHS) is with respect to x and integration with respect to t, (5) can be re-written to become

$$c^2 \frac{\partial^2}{\partial x^2} \int_0^\infty u e^{-st} dt = \int_0^\infty \frac{\partial^2 u}{\partial t^2} e^{-st} dt \tag{6}$$

It should be noted that the integrals of the LHS and RHS are simply the Laplace transforms of $u(x,t)$ and $\frac{\partial^2}{\partial t^2}u(x,t)$ respectively. If $\mathcal{L}[u(x,t)] = \bar{u}(x,s)$ is used to denote the Laplace transform of $u(x,t)$, equation (6) becomes

$$c^2\frac{\partial^2}{\partial x^2}\bar{u}(x,s) = s^2\bar{u}(x,s) - su(x,0) - \dot{u}(x,0) \tag{7}$$

Where $u(x,0) = u(x,t)\big)_{t=0}$ and $\dot{u}(x,0) = \frac{\partial}{\partial t}u(x,t)\big)_{t=0}$ are the initial conditions of the rod. Since steady state response is of interest in the present analysis, the initial conditions are zero; $u(x,0) = 0$ and $\dot{u}(x,0) = 0$ such that equation (7) becomes

$$c^2\frac{\partial^2}{\partial x^2}\bar{u}(x,s) = s^2\bar{u}(x,s) \tag{8}$$

Solution of (8) straight-forwardly becomes

$$\bar{u}(x,s) = A_1e^{xs/c} + A_2e^{-xs/c} \tag{9}$$

The boundary conditions of the bar are imposed by considering the quantity of force at the two ends of the bar. At the left end of the bar where $x = 0$ elasticity gives

$$AE\frac{\partial u}{\partial x}\Big)_{x=0} = AE\frac{\partial}{\partial x}u(0,t) = F(t) \tag{10}$$

At the right end of the bar where $x = l$ elasticity gives

$$\frac{\partial u}{\partial x}\Big)_{x=l} = \frac{\partial}{\partial x}u(l,t) = 0 \tag{11}$$

The Laplace transform of (10) goes as follows

$$AE\int_0^\infty \frac{\partial u(0,t)}{\partial x}e^{-st}dt = \int_0^\infty F(t)e^{-st}dt \tag{12}$$

$$AE\frac{\partial}{\partial x}\int_0^\infty u(0,t)e^{-st}dt = \int_0^\infty F(t)e^{-st}dt \tag{13}$$

These become

$$\frac{\partial}{\partial x}\bar{u}(0,s) = \frac{\bar{F}(s)}{AE} \tag{14}$$

From (9) results

$$\frac{\partial}{\partial x}\bar{u}(x,s) = A_1(s/c)e^{xs/c} - A_2(s/c)e^{-xs/c} \tag{15}$$

Making use of equations (11), (14) and (15) gives the two equations

$$A_1e^{ls/c} - A_2e^{-ls/c} = 0 \tag{16}$$

$$A_1 - A_2 = (c/s)\frac{\bar{F}(s)}{AE} \tag{17}$$

From which results

$$A_2 = \frac{-(c/s)\bar{F}(s)}{(1-e^{-2ls/c})AE} \tag{18}$$

$$A_1 = \frac{(c/s)e^{-2ls/c}\bar{F}(s)}{(e^{-2ls/c}-1)AE} \tag{19}$$

Putting (18) and (19) in (9) gives

$$\bar{u}(x,s) = \frac{-(c/s)\bar{F}(s)}{(1-e^{-2ls/c})AE}\left[e^{-2ls/c}e^{xs/c} + e^{-xs/c}\right]$$

which is further simplified to become

$$\bar{u}(x,s) = \frac{-(c/s)e^{-ls/c}\bar{F}(s)}{(1-e^{-2ls/c})AE}\left[e^{(s/c)(x-l)} + e^{(s/c)(l-x)}\right]$$

The above is re-arranged to be in the form required

$$\bar{u}(x,s) = \frac{-c\bar{F}(s)e^{-s(l/c)}}{sAE\left(1-e^{-2s(l/c)}\right)}\left[e^{(s/c)(x-l)} + e^{-(s/c)(x-l)}\right] \tag{20}$$

The inverse Laplace transform of (20) gives the solution of (4). The inverse Laplace transform of $[\bar{u}(x,s)]$ is given by the *Bromwich integral*

$$u(x,t) = \mathcal{L}^{-1}[\bar{u}(x,s)] = \int_{\lambda-i\infty}^{\lambda+i\infty} e^{st}\bar{u}(x,s)ds \tag{21}$$

The *Bromwich integral* is evaluated through the use of the *Residue theorem*

$$\oint_C \bar{u}(x,s)ds = 2\pi i\sum_j R_j \tag{22}$$

Where R_j is the residue at the jth pole of $\bar{u}(x,s)$ within the closed contour C. putting the exponential term in the denominator of $\bar{u}(x,s)$ in Maclaurin series gives that $\bar{u}(x,s)$ has infinitely many number of poles thus application of the residue theorem will be extremely difficult. Nevertheless, $\mathcal{L}^{-1}[\bar{u}(x,s)] = u(x,t)$ is computed through clever mathematical manipulations. Equation (20) is re-written as

$$\bar{u}(x,s) = \frac{-c\bar{F}(s)}{sAE}\frac{e^{(sl/c)(x/l-1)} + e^{-(sl/c)(x/l-1)}}{e^{(sl/c)} - e^{-(sl/c)}} \tag{23}$$

Since $s = i\omega$ equation (23) becomes

$$\bar{u}(x,s) = \frac{-c\bar{F}(s)}{i\omega AE}\frac{e^{(i\omega l/c)(x/l-1)} + e^{-(i\omega l/c)(x/l-1)}}{e^{(i\omega l/c)} - e^{-(i\omega l/c)}} \tag{24}$$

Further, equation (24) is re-arranged to

$$\bar{u}(x,s) = \frac{c\bar{F}(s)}{\omega AE}\frac{\left[e^{(i\omega l/c)(x/l-1)} + e^{-(i\omega l/c)(x/l-1)}\right]/2}{\left[e^{(i\omega l/c)} - e^{-(i\omega l/c)}\right]/2i} \tag{25}$$

From the theory of complex numbers it is recognized that $\left[e^{(i\omega l/c)(x/l-1)} + e^{-(i\omega l/c)(x/l-1)}\right]/2 = \cos[(\omega l/c)(x/l-1)]$ and $\left[e^{(i\omega l/c)} - e^{-(i\omega l/c)}\right]/2i = \sin(\omega l/c)$ meaning that $\bar{u}(x,s)$ is simply given as

$$\bar{u}(x,s) = \frac{c\bar{F}(s)}{\omega AE}\frac{\cos[(\omega l/c)(x/l-1)]}{\sin(\omega l/c)} \tag{26}$$

The solution of (4) becomes

$$u(x,t) = \frac{c}{\omega AE}\frac{\cos[(\omega l/c)(x/l-1)]}{\sin(\omega l/c)}\mathcal{L}^{-1}[\bar{F}(s)] = \frac{c}{\omega AE}\frac{\cos[(\omega l/c)(x/l-1)]}{\sin(\omega l/c)}F(t) \quad (27)$$

Equation (27) describes the steady state response of the slender rod to the excitation $F(t)$ derived in the s-domain.

3. Application to Harmonically Excited System

3.1. Vibration analysis

For the special case when $F(t) = F_0 e^{i\omega t}$ equation (27) gives

$$u(x,t) = \frac{c}{\omega AE}\frac{\cos[(\omega l/c)(x/l-1)]}{\sin(\omega l/c)}F_0 e^{i\omega t} \quad (28)$$

which is identical with the given result; $u(x,t) = \frac{cF_0 e^{i\omega t}\cos[(\omega l/c)(x/l-1)]}{\omega AE\sin(\omega l/c)}$. For validity, response of the slender rod $u(x,t)$ to the excitation $F(t)$ has to be derived in the t-domain and compared with (28) derived in the s-domain. On the t-domain the general solution of (4) has any of the forms

$$u(x,t) = A_1(t)\cos(\omega x/c) + A_2(t)\sin(\omega x/c) \quad (29a)$$

$$u(x,t) = [B_1\cos(\omega x/c) + B_2\sin(\omega x/c)]F(t) \quad (29b)$$

Equation (29b) assumes that the steady state response of the rod is of same form as the excitation which is the preponderant notion in literature while the form of Equation (29a) is not yet seen in the reviewed literature. Substituting in turn the boundary conditions (10) and (11) into (29) respectively gives the pair

$$A_1(t) = \frac{c}{\omega AE}\frac{\cos(\omega l/c)}{\sin(\omega l/c)}F(t), \quad A_2(t) = \frac{c}{\omega AE}F(t) \quad (30a)$$

$$B_1 = \frac{c}{\omega AE}\frac{\cos(\omega l/c)}{\sin(\omega l/c)}, \quad B_2 = \frac{c}{\omega AE} \quad (30b)$$

Substituting any of (30a) and (30b) into the corresponding general equation gives

$$u(x,t) = \frac{c}{\omega AE}\left[\frac{\cos(\omega l/c)\cos(\omega x/c)}{\sin(\omega l/c)} + \sin(\omega x/c)\right]F(t) \quad (31a)$$

$$u(x,t) = \frac{c}{\omega AE}\left[\frac{\cos(\omega l/c)\cos(\omega x/c)+\sin(\omega l/c)\sin(\omega x/c)}{\sin(\omega l/c)}\right]F(t) \quad (31b)$$

$$u(x,t) = \frac{c}{\omega AE}\left\{\frac{\cos[(\omega l/c)(x/l-1)]}{\sin(\omega l/c)}\right\}F(t) \quad (32)$$

Equation (32) is the required solution and seen to be identical with (27) thus validating the s-domain analysis. For the studied case where $F(t) = F_0 e^{i\omega t}$ equation (32) gives the required result

$$u(x,t) = \frac{cF_0 e^{i\omega t}\cos[(\omega l/c)(x/l-1)]}{\omega AE\sin(\omega l/c)} \quad (33)$$

Since generally excitation and response are related through the frequency response function $H_{u(x,t)}(\omega)$ by the equation; $u(x,t) = H_{u(x,t)}(\omega)F_0 e^{i\omega t}$ then

$$H_{u(x,t)}(\omega) = \frac{c\cos[(\omega l/c)(x/l-1)]}{\omega AE\sin(\omega l/c)} \quad (34)$$

3.2. Stress analysis

The stress is given by

$$\sigma(x,t) = E\frac{\partial}{\partial x}u(x,t) = -E\frac{c}{\omega AE}\frac{\omega}{c}\frac{\sin[(\omega l/c)(x/l-1)]}{\sin(\omega l/c)}F(t)$$

This simplifies to

$$\sigma(x,t) = \frac{-\sin[(\omega l/c)(x/l-1)]}{A\sin(\omega l/c)}F(t) \quad (35)$$

For the present case where $F(t) = F_0 e^{i\omega t}$, stress reads

$$\sigma(x,t) = \frac{-\sin[(\omega l/c)(x/l-1)]}{A\sin(\omega l/c)}F_0 e^{i\omega t} \quad (36)$$

Similarly the frequency response function of the harmonic internal stress is $H_{\sigma(x,t)}(\omega)$ by the equation;

$$H_{\sigma(x,t)}(\omega) = \frac{-\sin[(\omega l/c)(x/l-1)]}{A\sin(\omega l/c)} \quad (37)$$

4. Numerical Simulation and Discussion

For the purpose of numerical simulation of problems, the slender rod is chosen to be made of stainless steel (18-8) materials with the physical constants; Modulus of elasticity E =190 GPa and mass density ρ=7747.19674. The slender rod has radius r =1cm and length l=2m. The excitation force is $F(t) = 1000e^{i10t}$.

4.1. Numerical vibration analysis

Three dimensional graphical analysis of $H_{u(x,t)}(\omega)$ plotted against the plane of ω and x is shown in figure1. It is seen from figure1 that $H_{u(x,t)}(\omega)$ responds steeply with changes in ω but responds only slightly to changes in x.

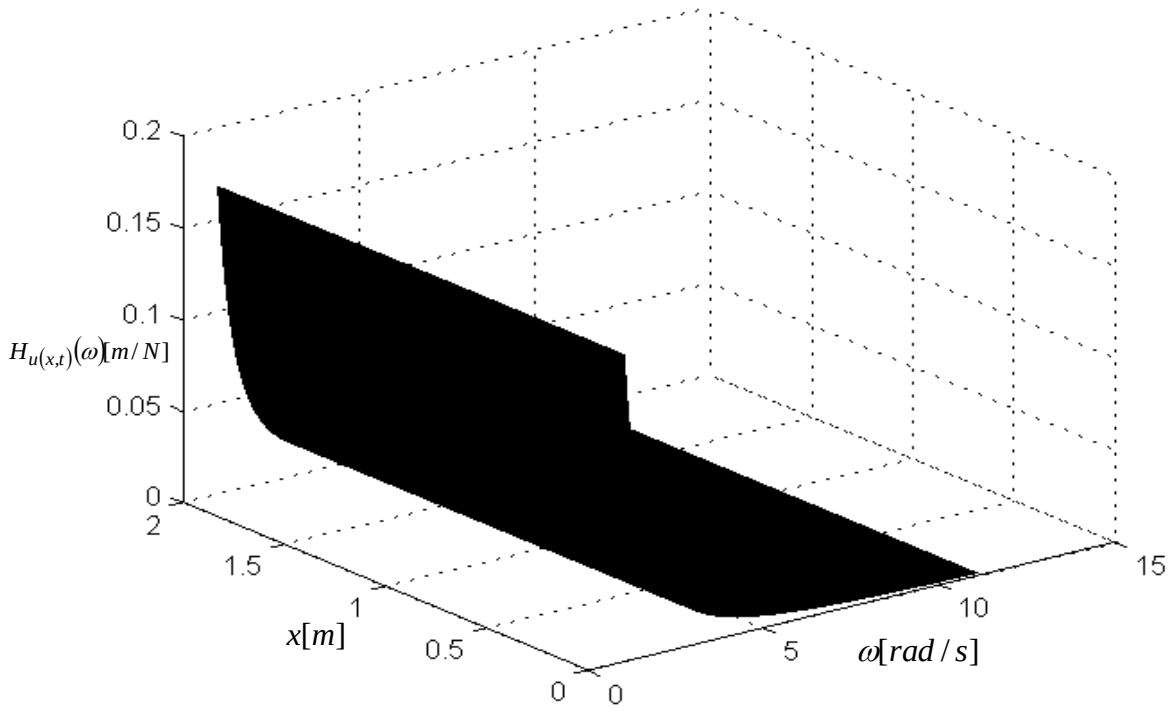

Figure1. Variation of $H_{u(x,t)}(\omega)$ with ω along x

Graphical analysis of (33) requires that $u(x,t)$ be written out as

$$u(x,t) = Re[u(x,t)] + iIm[u(x,t)] \quad (38)$$

Where the real part of $u(x,t)$ given as

$$Re[u(x,t)] = F_0 H_{u(x,t)}(\omega)\cos(\omega t) \quad (39a)$$

is response of the system to the excitation $F(t) = F_0\cos(\omega t)$ while the imaginary part of $u(x,t)$ given as

$$Im[u(x,t)] = F_0 H_{u(x,t)}(\omega)\sin(\omega t) \quad (39b)$$

is response of the system to the excitation $F(t) = F_0\sin(\omega t)$. Graphical analysis of equations (39a) and (39b) when $F_0 = 1000$ and $\omega = 10$ are given as Figure2 and Figure3 respectively. Figure2a is a surface plot of that shows variation of $Re[u(x,t)]$ with simultaneous variation in t and x. The shape of response of the slender bar to $F(t) = 1000\cos(\omega t)$ designated $Re[u(x,t)]$ is given in figure2b. Each component shape of figure2b is titled by the time at which the shape occurs. It should be noted from Figure2b that the response $Re[u(x,t)]$ is periodic since shapes at $t = T = 2\pi/\omega$ and $t = 2T$ are identical. Figure3a is a surface plot of that shows variation of $Im[u(x,t)]$ with simultaneous variation in t and x. The shape of response of the slender bar to $F(t) = 1000\sin(\omega t)$ designated $Im[u(x,t)]$ is given in figure3b. It should also be noted from Figure3b that the response $Im[u(x,t)]$ is periodic since shapes at $t = T = 2\pi/\omega$ and $t = 2T$ are identical.

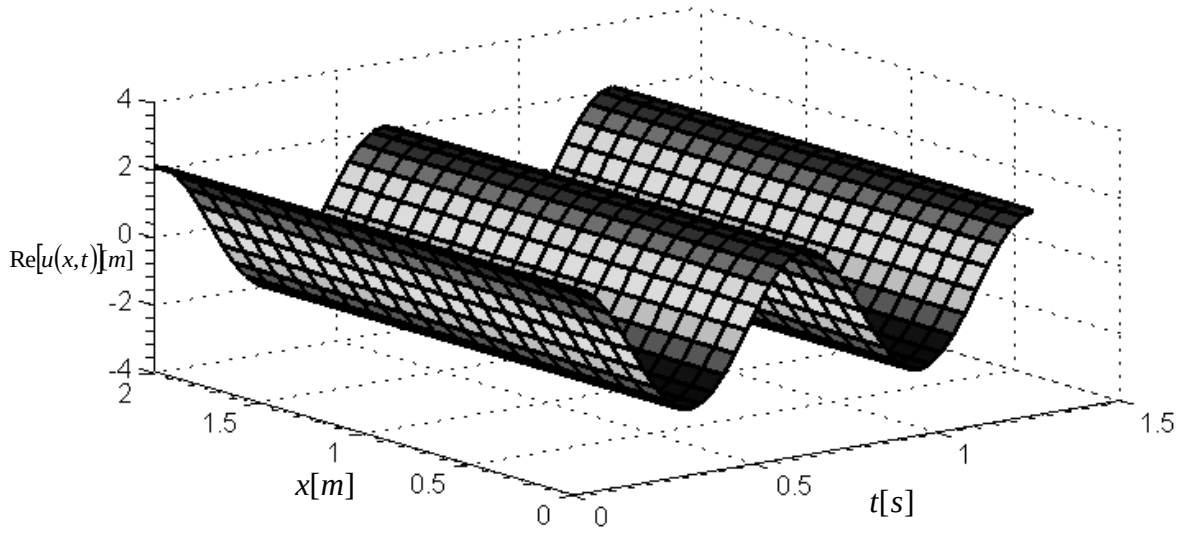

Figure2a. Surface that shows variation of $Re[u(x,t)]$ with simultaneous variation of t and x

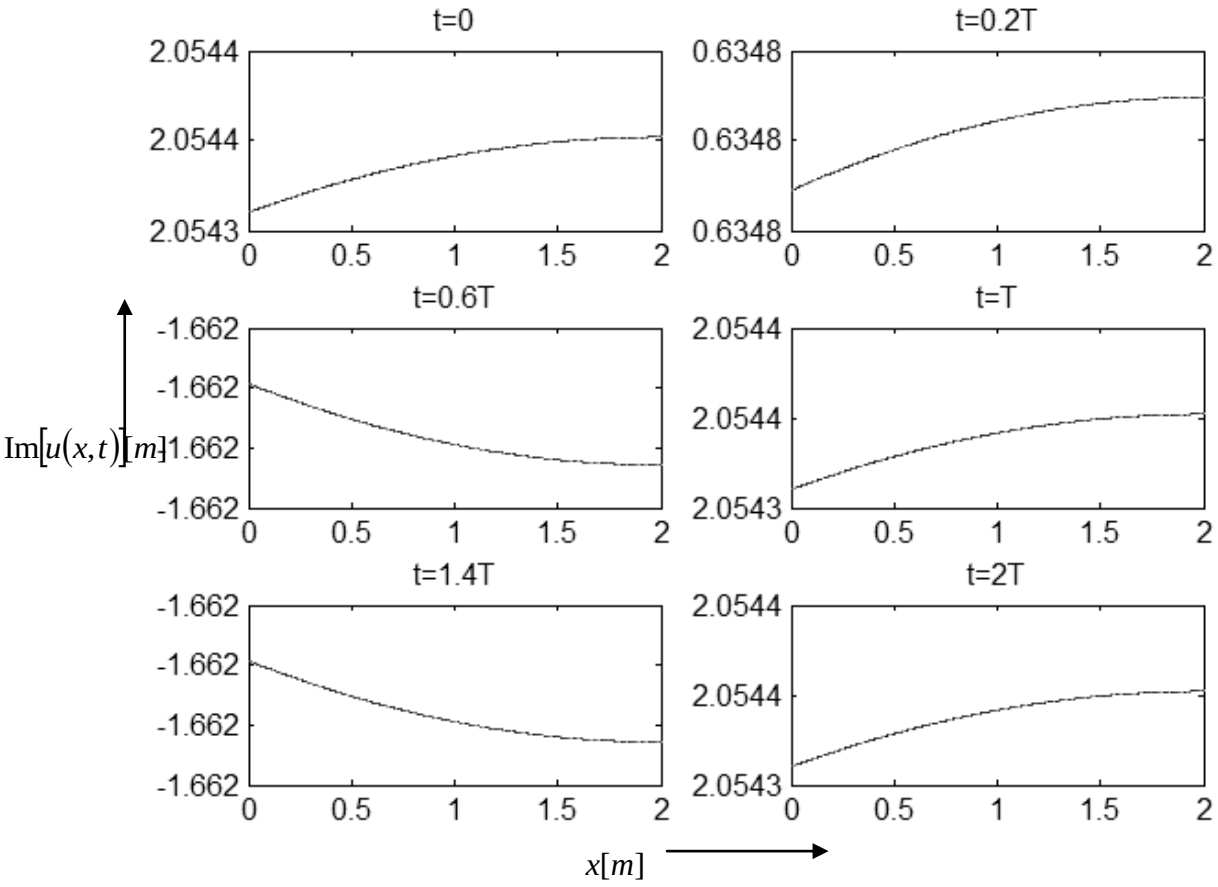

Figure2b. The shape of response $Re[u(x,t)]$ along the axis of the slender bar.

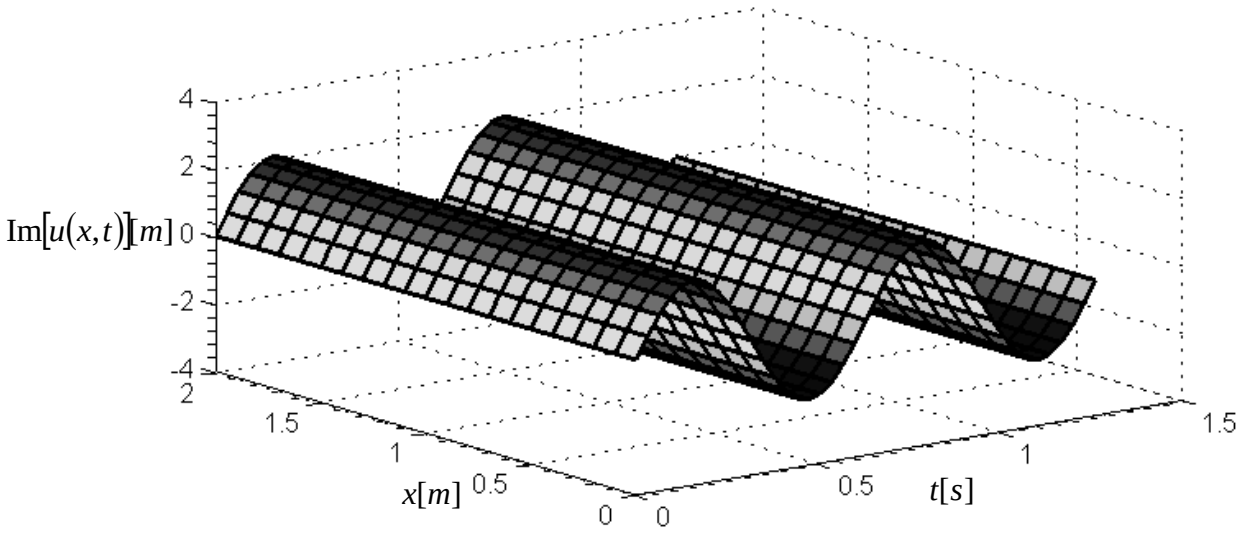

Figure3a. Surface that shows variation of $Im[u(x,t)]$ with simultaneous variation of t and x

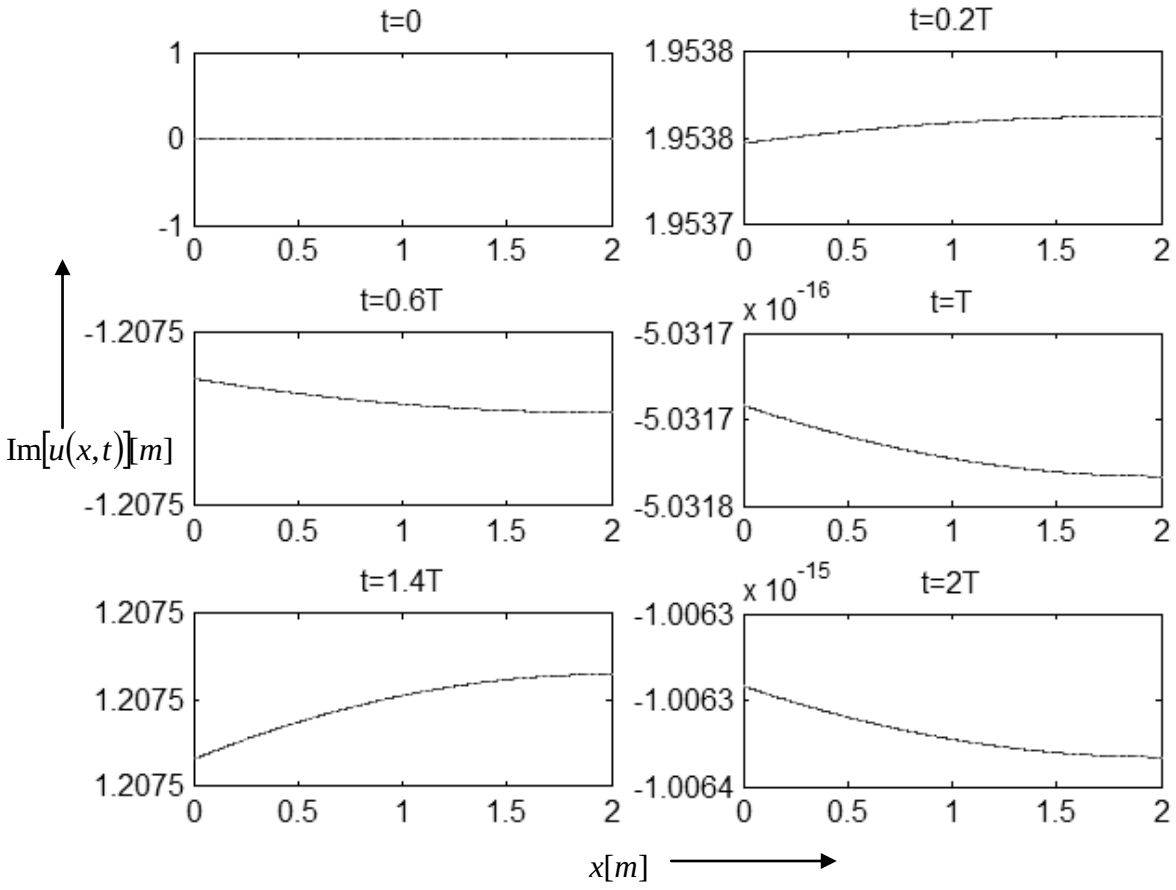

Figure3b. The shape of response $Im[u(x,t)]$ along the axis of the slender bar.

Graphical analysis of $Re[u(x,t)]$ and $Im[u(x,t)]$ as function of circular frequency ω are given in Figures4 and 5 respectively. Figure4a is a surface plot that shows variation of $Re[u(x,t)]$ with simultaneous variation in ω and x. Each component of figure4b is titled with the time at which it occurs. Figure5a is a surface plot of that shows variation of $Im[u(x,t)]$ with simultaneous variation in ω and x. The side views of the surface plots of Figures4a and 5a at $x = 1$ are shown in figures 4b and 5b. It is seen from both figures4 and 5 that dependence of response $u(x,t)$ on ω decays with rise in ω.

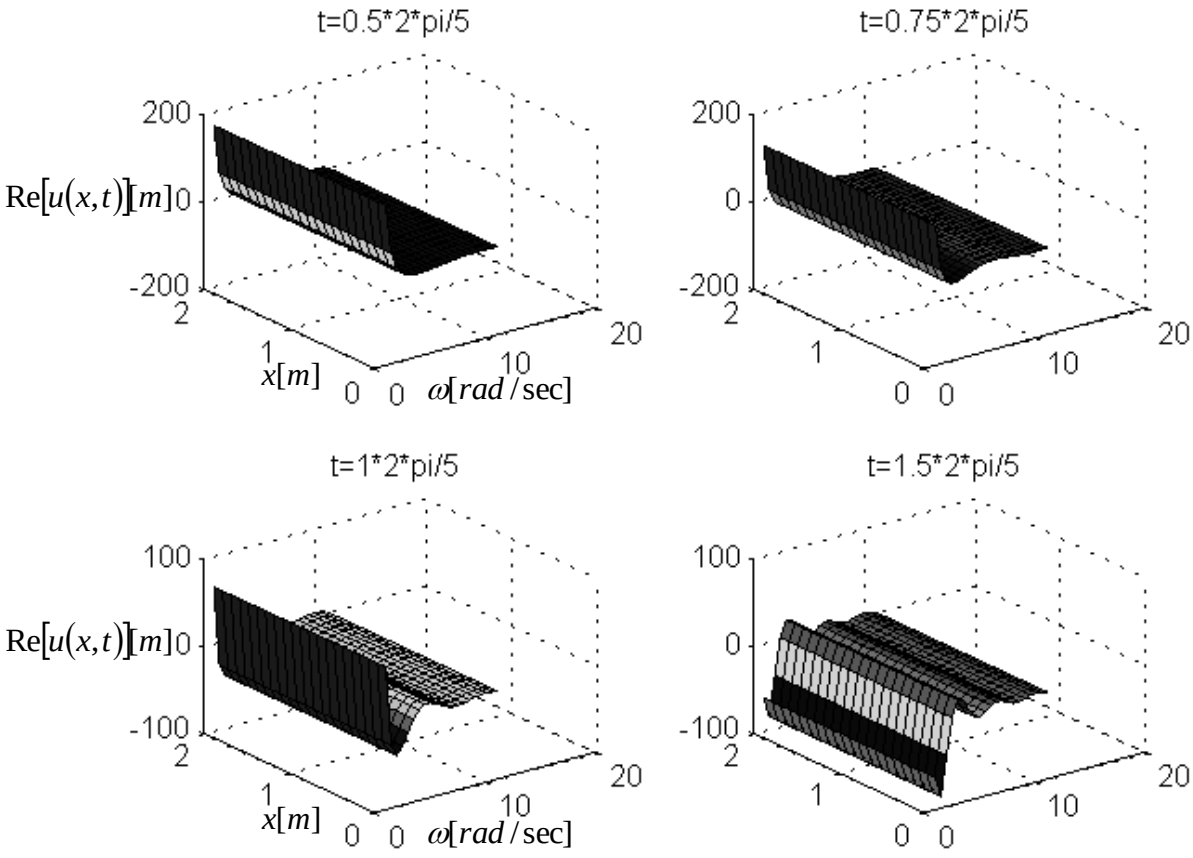

Figure4a. Surface plot of $Re[u(x,t)]$ against ω and x

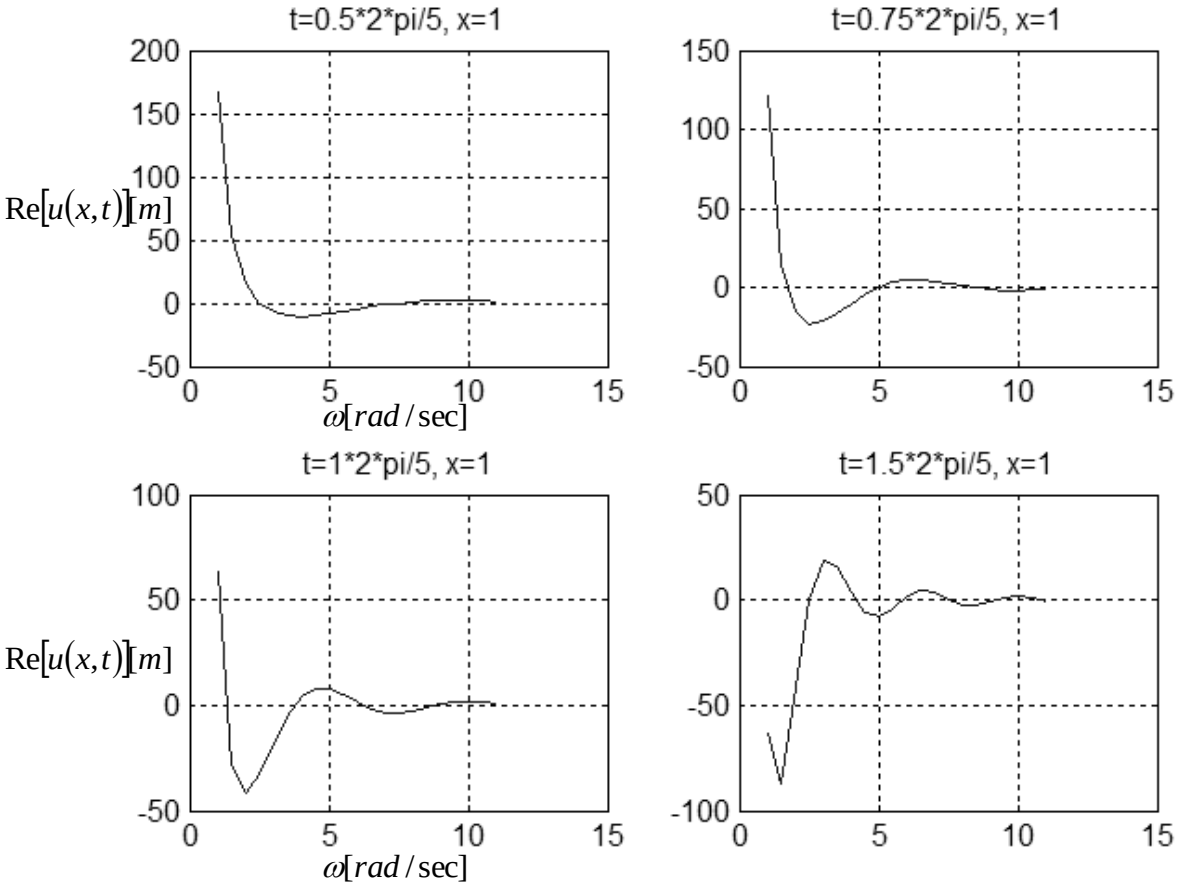

Figure4b. Line plot of $Re[u(x,t)]$ against ω at $x = 1$m and values of t shown in the title

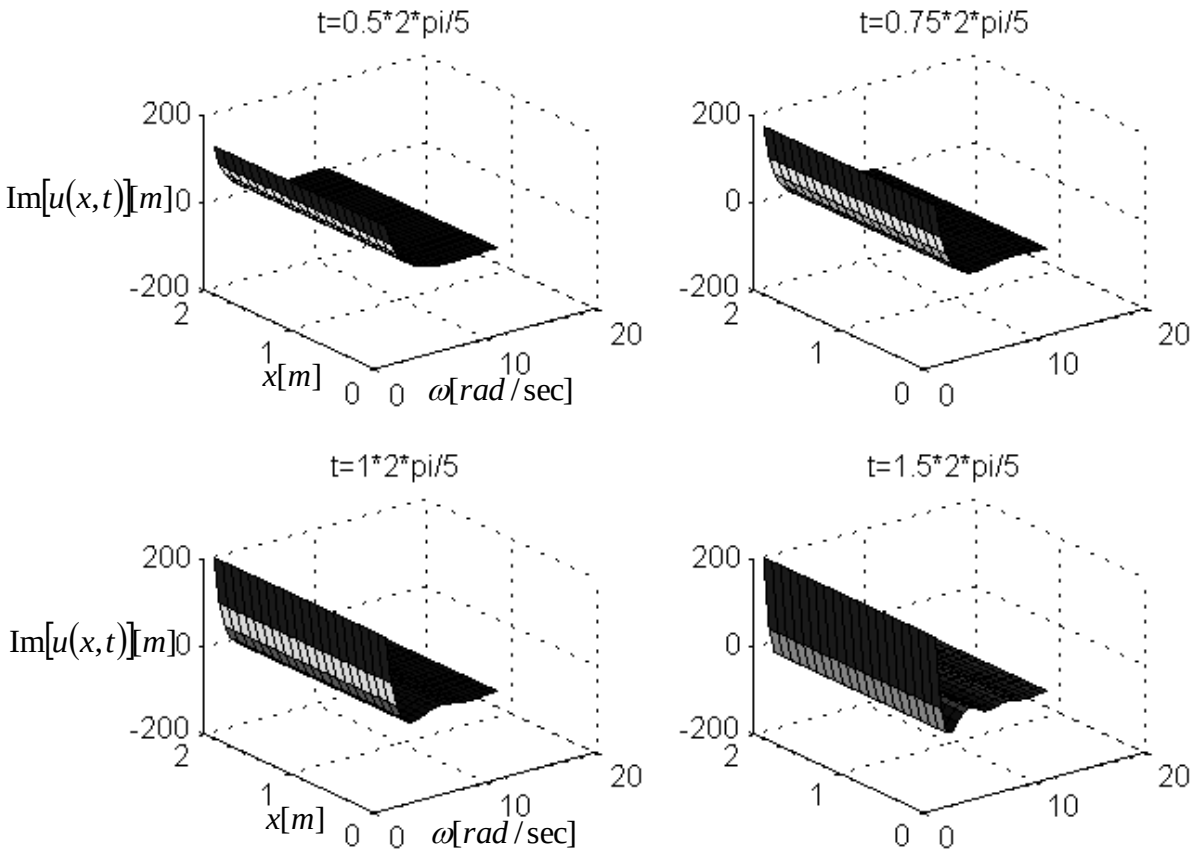

Figure5a. Surface plot of $Im[u(x,t)]$ against ω and x

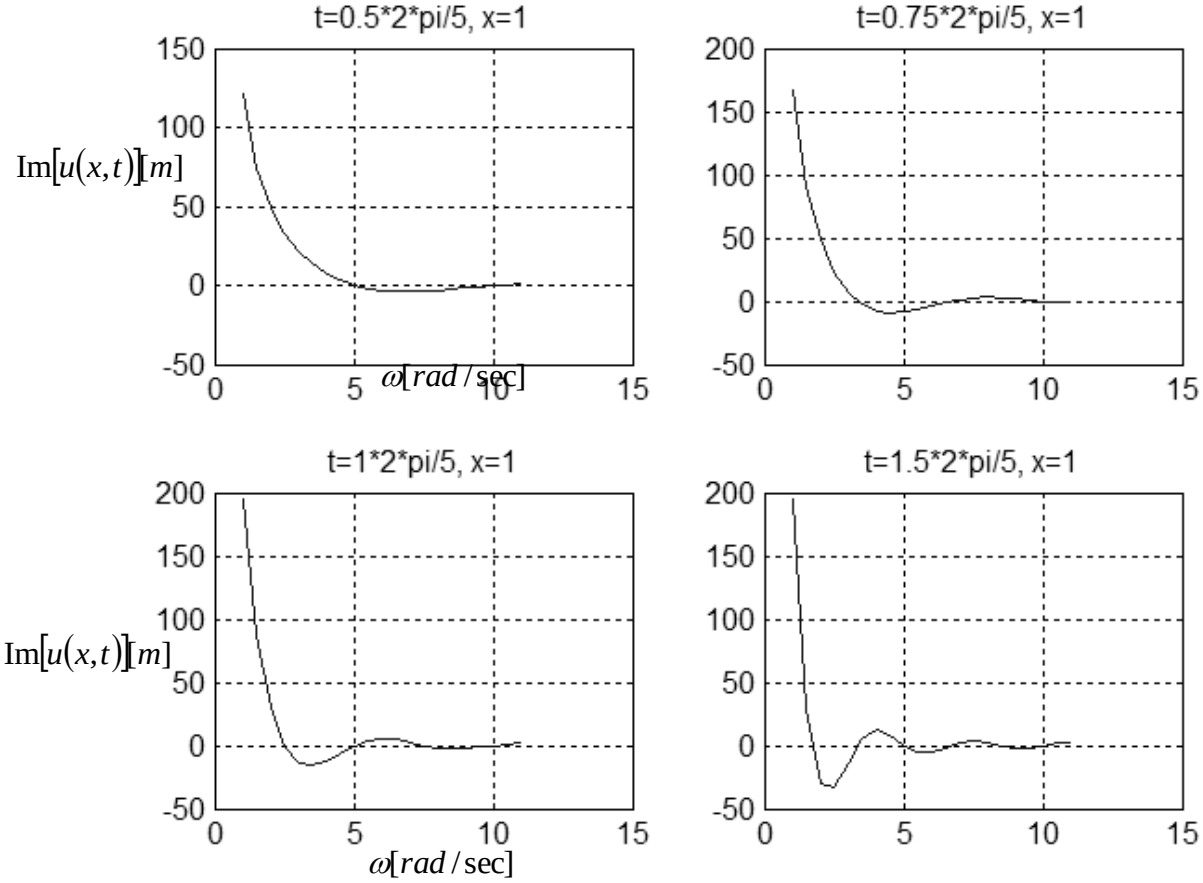

Figure5b. Line plot of $Im[u(x,t)]$ against ω at $x = 1$m and values of t shown in the title

4.2. Numerical stress analysis

Graphical analysis of (36) requires that $\sigma(x,t)$ be written as

$$\sigma(x,t) = Re[\sigma(x,t)] + iIm[\sigma(x,t)] \quad (40)$$

Where the real part of $\sigma(x,t)$ given as

$$Re[\sigma(x,t)] = F_0 H_{\sigma(x,t)}(\omega)\cos(\omega t) \quad (41a)$$

is the internal harmonic stress of the rod to the excitation $F(t) = F_0\cos(\omega t)$ while the imaginary part of $\sigma(x,t)$ given as

$$Im[\sigma(x,t)] = F_0 H_{\sigma(x,t)}(\omega)\sin(\omega t) \quad (41b)$$

is the internal harmonic stress of the rod to the excitation $F(t) = F_0\sin(\omega t)$. Graphical analysis of equations (41a) and (41b) when $F_0 = 1000$ and $\omega = 10$ are given as Figure6 and Figure7 respectively. Figure6 is a surface plot that shows variation of $Re[\sigma(x,t)]$ with simultaneous variation in t and x while Figure7 is a surface plot of that shows variation of $Im[\sigma(x,t)]$ with simultaneous variation in t and x. It is seen that both graphical results agree with the boundary condition that stress at the free end $(x = l)$ of the bar is zero. The maximum amplitude of fluctuation of internal stress occurs at $x = 0$ where force is applied. It is seen from figures8 and 9 that dependence of response $\sigma(x,t)$ on ω is periodic unlike dependence of $u(x,t)$ on ω that decays with rise in ω. The difference in dependence of $\sigma(x,t)$ and $u(x,t)$ on ω is easily understood when the mathematical forms of $H_{\sigma(x,t)}(\omega)$ and $H_{u(x,t)}(\omega)$ are compared. It is seen that the differences arise from the fact that $H_{u(x,t)}(\omega)$ has both trigonometric and inverse relationship with ω while $H_{\sigma(x,t)}(\omega)$ has only trigonometric relationship with ω. The excited end of the rod can be considered the base of the rod from which excitation is longitudinally transmitted to the rod. This means that the base should be the focus of design against fatigue. This work could have practical application when a blade attached to an unbalanced shaft is to be investigated.

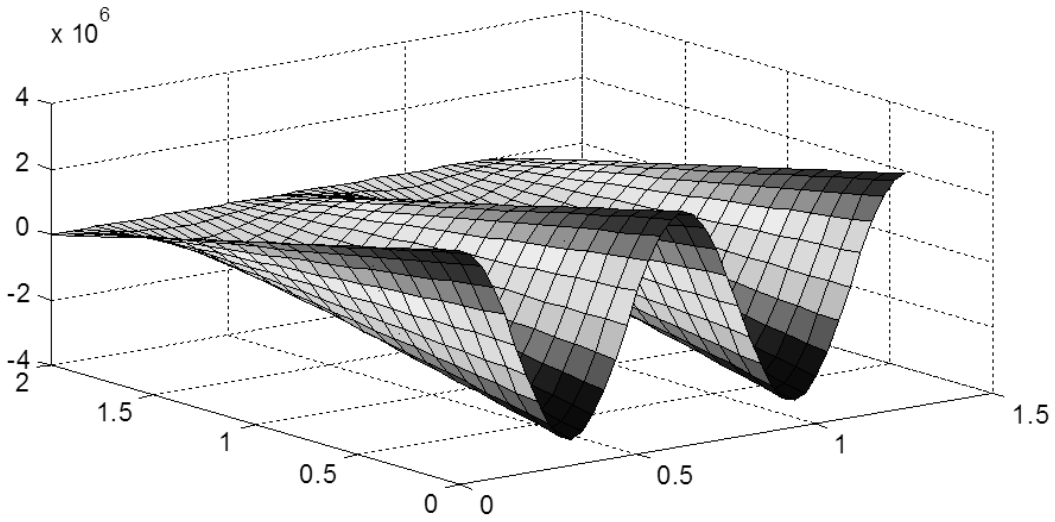

Figure6. Surface that shows variation of $Re[\sigma(x,t)]$ with simultaneous variation of t and x

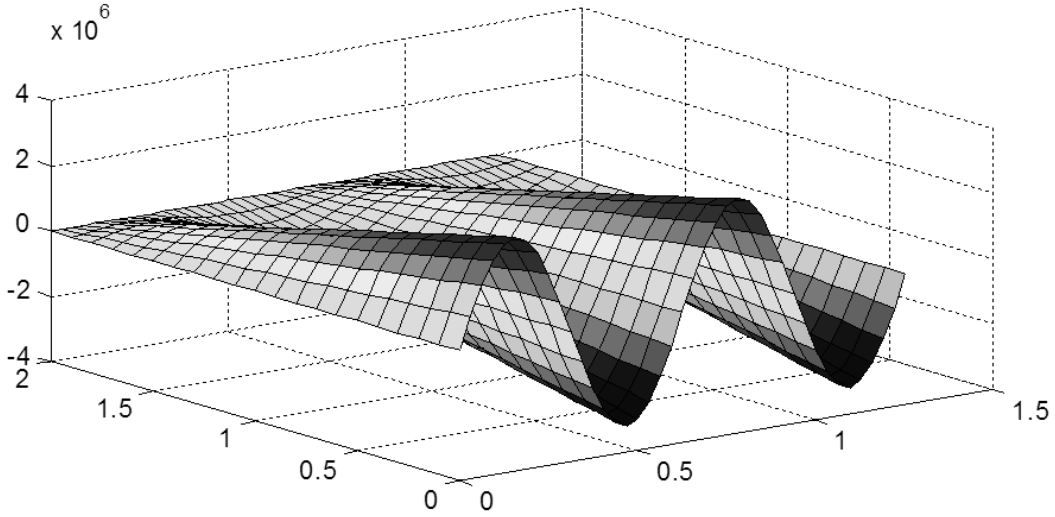

Figure7. Surface that shows variation of $Im[\sigma(x,t)]$ with simultaneous variation of t and x.

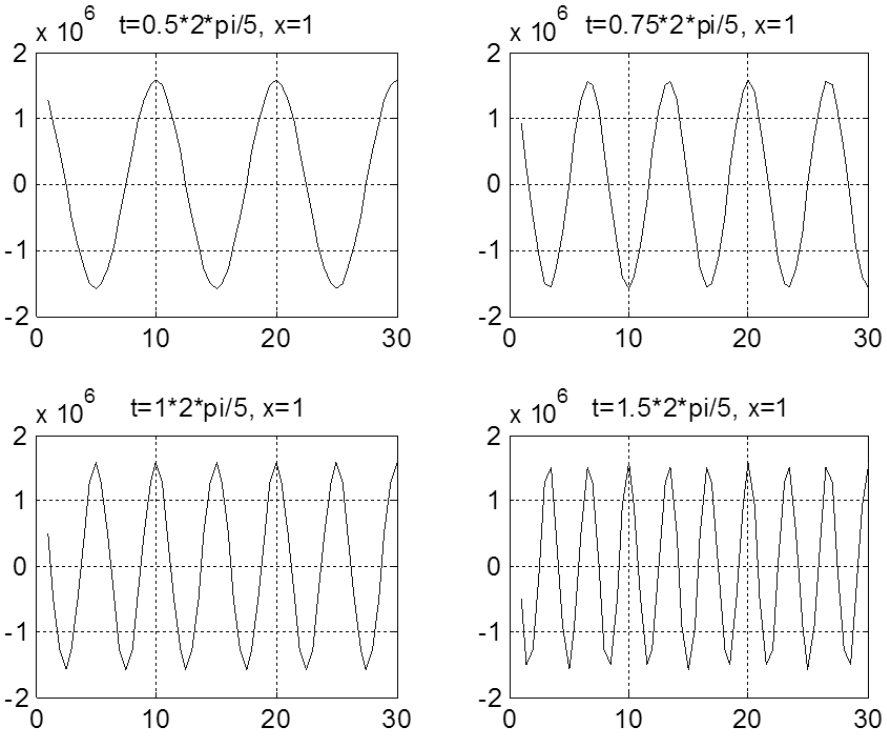

Figure8. Line plot of $Re[\sigma(x,t)]$ against ω at $x = 1$m and values of t shown in the title

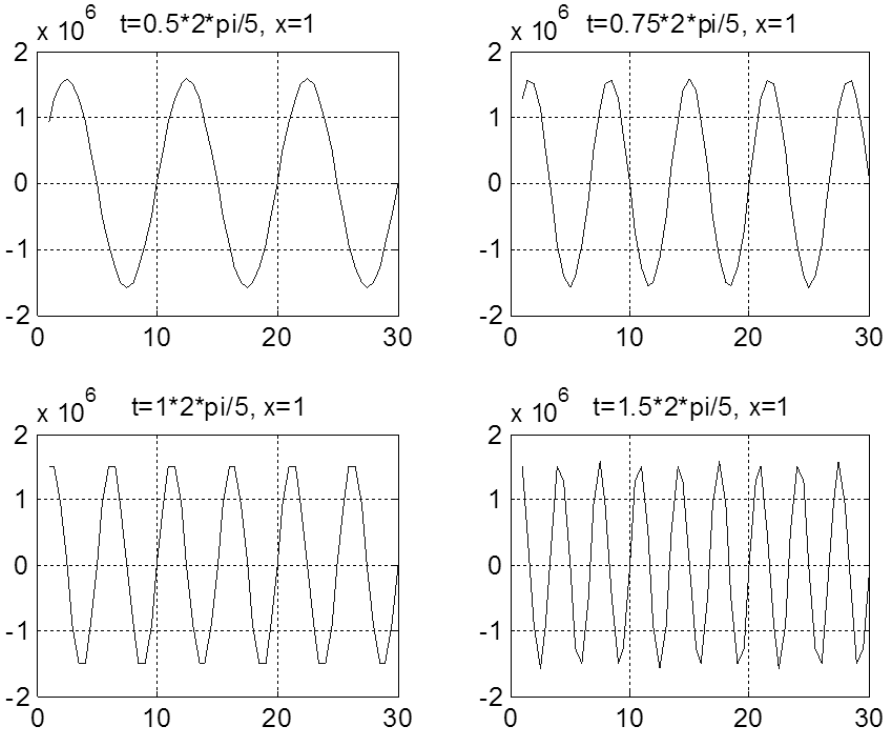

Figure9. Line plot of $Im[\sigma(x,t)]$ against ω at $x = 1$m and values of t shown in the title

5. Conclusion

Vibration of a uniform slender bar modelled as continuum is analyzed on the Laplace variable domain. The method of separation of variables is used to validate the results. A novel form of the method of separation of variables is used and seen to conform with the popular form that assumes that the steady state response of the rod is of same form as the forcing function. Numerical simulation of vibratory responses of displacement and stress are presented and discussed. It is seen that the excitation frequency ω affects the displacement $u(x,t)$ and the internal stress differently. The displacement $u(x,t)$ of a point on the rod for a frozen time decays with rise in ω. But on the other hand dependence of stress $\sigma(x,t)$ on ω is periodic with fixed amplitude. This means that a rise in ω is expected to cause deformation of a point to fall but has no effect on the stress amplitude. This can also be interpreted to mean that even though deformation of a point falls with rising circular frequency, the amplitude of fatigue load is unaffected. The difference in response of $\sigma(x,t)$ and $u(x,t)$ to variation in ω arises from the fact that $H_{u(x,t)}(\omega)$ has both trigonometric and inverse relationship with ω while $H_{\sigma(x,t)}(\omega)$ has only trigonometric relationship with ω. Numerical results are seen to agree with the boundary condition that stress amplitude at the free end ($x = l$) and excited end of the bar ($x = 0$) are respectively zero and non-zero (maximum). Practical application of analysis is proffered to include the case of blades attached to an unbalanced shaft.

REFERENCES

[1]. S. S. Rao, *Mechanical Vibrations*(4th ed.),Dorling Kindersley, India, 2004.

[2]. P. L.Gatti and V. Ferrari, Applied Structural and Mechanical Vibrations: Theory, methods and measuring instrumentation, Taylor & Francis e-Library, 2003.

[3]. S. G. Kelly, *Mechanical Vibrations: Schaum's Outline Series*, McGraw-Hill, 1996.

[4]. R. F. Steidel, Jr., *An Introduction to Mechanical Vibrations* (4th ed.), Wiley, New York, 1989.

[5]. A. D. Dimarogonas, *Vibration Engineering*, West Publishing, Saint Paul, MN, 1976.

[6]. S. Timoshenko, D. H. Young, and W. Weaver, Jr., *Vibration Problems in Engineering* (4th ed.), Wiley, New York, 1974.

[7]. M. Paz, *Structural Dynamics: Theory and Computation* (2nd ed.), Van Nostrand Reinhold, New York, 1985.